

A theoretical analysis of Ballistic Electron Emission Microscopy: k-space distributions and spectroscopy.

P.L. de Andres

Instituto de Ciencia de Materiales (CSIC), Cantoblanco, E-28049 Madrid (SPAIN)

K. Reuter

Lehrstuhl für Festkörperphysik, University of Erlangen-Nürnberg (Germany)

F.J. Garcia-Vidal, D. Sestovic and F. Flores

Dept. de Física Teórica de la Materia Condensada (UAM), Universidad Autónoma de Madrid,

E-28049 Madrid (SPAIN)

(May 26, 2017)

Abstract

We present a theoretical framework well suited to analyze Ballistic Electron Emission Microscopy (BEEM) experiments. At low temperatures and low voltages, near the threshold value of the Schottky barrier, the BEEM current is dominated by the elastic component. Using a Keldysh Green's functions method, we analyze the injected distribution of electrons and the subsequent propagation through the metal. Elastic scattering by the lattice results in the formation of focused beams and narrow lines in real space. To obtain the current injected in the semiconductor, we compute the current distribution in reciprocal space and, assuming energy and k_{\parallel} conservation, we match states to the projected conduction band minima of the semiconductor. Our results show an important focalization of the injected electron beam and explain the similarity between BEEM currents for Au/Si(111) and Au/Si(100).

I. INTRODUCTION

Among the many exciting applications of the Scanning Tunneling Microscope (STM) one has recently become established as a technique in its own: Ballistic Electron Emission Microscopy (BEEM)^{1,2}. In the standard version of this technique, the STM acts as a microscopic gun injecting a very narrow and coherent beam of electrons on a metallic layer deposited on a semiconductor. The electrons are subsequently propagated through the metallic layer and finally are detected in the semiconductor, passed the metal-semiconductor interfacial Schottky barrier. Both, spectral resolution and a lateral nanometric geometrical resolution, allow a detailed study of the buried interface that cannot be easily obtained by other techniques. Besides the interest of obtaining accurate information on the metal-semiconductor interface, other processes of technological importance have a considerable influence on the final BEEM current, and can be studied by applying this technique. A relevant example is the current attenuation length, determined by various inelastic processes: clearly these quantities are of paramount importance to design and operate very small devices.

The main obstacle on this road is just the complexity of the technique itself. The general case is that many different physical processes contribute in quite different ways to the BEEM current, resulting in a complex mixing of interfering effects that preclude an easy determination of each of them separately. The only way out is to construct a realistic theory that can reliably handle each factor, trying to avoid spurious correlations of fitted values. Unfortunately, this is often the case when a parametrized approach, like the popular E-space Monte-Carlo technique, is applied to obtain different values related between them, transferring uncertainties and errors from one place to the other without control. In particular, the elastic interaction of electrons with the lattice has been described

as equivalent to a random walk, that cannot mimic the real interaction that is known to produce gaps in certain directions. Free propagation of carriers on distances of about 20 Å in forbidden directions are not desirable, but possible in those Monte-Carlo simulations. Also, the simulations are very sensitive to the initial tunneling distribution, that is taken into account only through planar tunneling theory and WKB approximation.

As mentioned before, an important capability of the technique is its ability to measure different attenuation lengths related to inelastic interactions. The main inelastic processes are the electron-electron and the electron-phonon interaction. Lowering the temperature to 77 K the electron-phonon interaction is already very low and one can ignore it to concentrate on the electron-electron interaction only. A very interesting result obtained using this approach is that the standard lifetime derived considering the dynamically screened Coulomb potential in an electron gas with a density related to gold cannot adequately explain the BEEM experiments³. This result seems independent of the particular set of parameters used in the E-space Monte-Carlo simulation, and has been also confirmed by fully *ab initio* k-space Monte-Carlo⁴. Because of the importance of this problem, we shall discuss it further in the context of our *ab initio* Green's function calculation.

In this paper we describe an *ab initio* Green's function calculation that can be used to compared with experimental results. In the pure elastic case (ballistic current) this formalism does not use any free parameter, while to take into account the inelastic electron-electron interaction we make use of a mean free path parametrization proposed by Bell³, that let us to choose a single value to get good agreement with experiments. We notice that this is a rather similar situation to other fields, like the Low Energy Electron Diffraction, where first principles Green's functions methods are supplemented with parametrized values of the imaginary part of the self-energy (typically a constant value) to include inelastic effects in the theory⁵. This approach has been proven succesful in those fields, and we hope it will introduce for BEEM a new way to compare theory and experiment. The paper is organized as follows: in section II we describe a theoretical framework covering three important steps on a BEEM experiment: the initial tunneling injection, the propagation of electrons through

the metallic layer, and the transmission of electrons at the two-dimensional plane defining the interface between the metal and the semiconductor. Finally, in section III, our theoretical results are compared with spectroscopic I(V) experimental data taken under conditions compatible with our main assumptions by other authors.

II. THEORY

Our theoretical approach is based on a hamiltonian describing separately the STM tip (T), the metal (M), and their interaction (I):

$$\hat{H} = \hat{H}_T + \hat{H}_M + \hat{H}_I \quad (1)$$

where the tip is defined by $\hat{H}_T = \sum \epsilon_\alpha \hat{n}_\alpha + \sum \hat{T}_{\alpha\beta} c_\alpha^\dagger c_\beta$, the metal is given by $\hat{H}_M = \sum \epsilon_i \hat{n}_i + \sum \hat{T}_{ij} c_i^\dagger c_j$, and the coupling term between them is $\hat{H}_I = \sum \hat{T}_{\alpha j} c_\alpha^\dagger c_j$ (where greek indexes, α, β , describe orbitals on the tip and latin indexes, i, j , refer to the metal). The interaction hamiltonian has been written in terms of a hopping matrix that couples the atomic orbitals in the tip with the atomic orbitals in the metal. Because for BEEM work the tip-sample distance is usually large, we make the approximation of considering only tunneling between s-orbitals. The hamiltonian describing the metal has been written on a tight-binding approximation with parameters given by Papaconstantopoulos⁶ for gold.

Currents between the tip and the sample and within the metal base are computed applying a Keldysh formalism⁷:

$$J_{ij} = \int d\omega Tr \{ \hat{T}_{ij} (\hat{G}_{ij}^{+-} - \hat{G}_{ji}^{+-}) \} \quad (2)$$

that is well suited for a non-equilibrium problem like the tunneling one, but also allow to write an elegant expresion for more standard scenarios like the propagation through the metal layer. The central objects in this formalism, \hat{G}_{ij}^{+-} , are obtained from a Dyson-like equation through the retarded and advanced Green functions of the uncoupled parts of the system (the tip and the sample), \hat{g}^R and \hat{g}^A , and the hopping matrix \hat{T} ^{8,9}. In that context,

it has been shown previously how the current between two atoms i, j in the metal can be obtained by:

$$J_{ij} = \frac{2e}{\pi\hbar} \Re \int_{-\infty}^{\infty} d\omega [f_T(\omega) - f_S(\omega)] \times Tr \sum_{m\alpha\beta n} [\hat{T}_{ij} \hat{g}_{jm}^R \hat{T}_{m\alpha} (\hat{g}_{\alpha\beta}^A - \hat{g}_{\alpha\beta}^R) \hat{T}_{\beta n} \hat{g}_{ni}^A] \quad (3)$$

where T_{ij} is the hopping matrix between atoms i, j , g_{jm}^r and g_{mj}^a are the retarded and advanced Green functions linking sites j and m , $(\hat{g}_{\alpha\beta}^A - \hat{g}_{\alpha\beta}^R)$ is related to the density of states matrix on the active atom at the tip (from now on assumed for simplicity to be 0), and the trace implies a summation over the orbitals forming the chosen basis. Eq. 3 describes the coherent propagation of electrons between the surface sites (m or n), and the atoms inside the crystal (i and j), and ingredient that we find of paramount importance to describe appropriately the BEEM current in the metal.

In this formalism the initial tunneling current is obtained as the current between the last atom in the tip (0) and all the atoms active for tunneling in the metal (m). In the same Keldysh formalism, we can write:

$$J_T = \int d\omega Tr \sum_m [\hat{T}_{0m} \hat{G}_{m0}^{+,-}(\omega) - \hat{T}_{m0} \hat{G}_{0m}^{+,-}(\omega)] \quad (4)$$

that for long tip-sample distances and the simpler case where only one atom is active for tunneling in the metal yields¹⁰:

$$J_T = \frac{4\pi e}{\hbar} \int_{-\infty}^{\infty} Tr [\hat{T}_{01} \hat{\rho}_{11}(\omega) \hat{T}_{10} \hat{\rho}_{00}(\omega)] [f_T(\omega) - f_S(\omega)] d\omega \quad (5)$$

where the further simplification of allowing tunneling to only one atom in the metal (m=1) has been made. This formula shows the dependence of the tunneling current with the hopping matrix linking the tip to the surface, T_{01} , the density of states at the two active sites, ρ_{00} and ρ_{11} , and the different Fermi distribution functions. This approach can be used to compute topographic images of a given surface (either at constant intensity or constant height) and already has been successfully used to compare with experiments¹¹.

The current distribution in reciprocal space is necessary to match wavefunctions across the metal-semiconductor interface in order to calculate the BEEM current in the semiconduc-

tor. It is possible to show that in k-space the current per energy unit between two layers a, b in the metal, is given by an expression formally identical to Eq. 3.:

$$J_{ab}(k_{\parallel}) = \frac{2e}{\pi\hbar} \Re Tr[\hat{T}_{ab}(k_{\parallel})\hat{g}_{b1}^R(k_{\parallel})\hat{T}_{10}\hat{\rho}_{00}\hat{T}_{01}\hat{g}_{1a}^A(k_{\parallel})] \quad (6)$$

where the various quantities are two-dimensional Fourier transforms of the respective objects appearing in the real space current between two nodes of the metallic lattice i, j :

$$\hat{T}_{i,j}(\vec{r}_{\parallel}) = \sum_{k_{\parallel}} e^{-i\vec{k}_{\parallel}\vec{r}_{\parallel}} \hat{T}_{a,b}(\vec{k}_{\parallel}) \quad (7)$$

The summation is performed over a set of special points covering the two-dimensional Brillouin zone¹².

A proper calculation of the quantum mechanical transmission coefficient, T , across the interface can be done by projecting and matching metal and semiconductor bulk states into the interface¹³. This procedure yields, as expected, a square root variation of that coefficient with the energy (measured w.r.t. the semiconductor conduction band minimum). Usually, a much easier model is applied in the literature where the transmission coefficient over a step-like potential barrier (taken as the Schottky barrier) is considered: this brings the correct behaviour with energy, but because this is a one-dimensional problem the variation of T with k_{\parallel} is not well represented. An intermediate level of sophistication, improving significantly the model, would be to describe the semiconductor within the Jones zone approximation and to match the wavefunctions logarithmic derivatives given a particular orientation for the semiconductor. In particular, this approach is quite reasonable around the semiconductor energy gap and can describe satisfactorily the region close to the conduction band minima. We have followed this approach using a Surface Green's function matching formalism^{14,15} (equivalent to the mentioned wave function matching), considering the neighbourhood of the projected $\Gamma - X$ direction (\overline{M}) in the Si(111) and Si(100) surfaces: these are the regions where the conduction band minima of Si are projected. In the parallel direction, where the kinematic restriction of conserving k_{\parallel} and having enough energy to be injected in the semiconductor is applied, a simple parabolic approximation with effective masses taken from

the literature is used. This defines an ellipsoidal region around the minimum of the semiconductor conduction band where the two-dimensional transmission coefficient described above changes continuously from its value at the center of the ellipse (the origin where the \vec{k}_{\parallel} is measured in the semiconductor) to zero at the boundaries of that region. This approach increases transmission at the interface by values between $\frac{15}{100}$ and $\frac{40}{100}$, depending on the energy.

For the particular case of a (111) orientation and in the neighbourhood of the \overline{M} point we have¹⁴:

$$\gamma = \frac{(1 - \frac{2}{3}hL)(1 - \frac{5}{6}hL)}{(1 + \frac{2}{3}hL)(1 + \frac{6}{6}hL)}$$

where $h = \frac{2\pi\sqrt{3}}{a}$, and $\frac{1}{L} = \sqrt{2(E - \frac{\kappa^2}{2})}$.

defining,

$$a = \frac{e - \frac{\kappa^2}{2} - v + \sqrt{(e - \frac{\kappa^2}{2})^2 - v^2}}{v}$$

with $v \approx 2eV$ to represent the silicon gap. Finally, the reflection amplitude is given by:

$$r = \frac{\frac{1+\gamma}{1-\gamma} - \frac{a-1}{a+1}}{\frac{1+\gamma}{1-\gamma} + \frac{a-1}{a+1}} \quad (8)$$

III. RESULTS

A. k-space and r-space distribution.

In this section, our formalism is applied to the case of Au grown on Si(111) or Si(100) orientations. From previous structural work performed with LEED, Auger and STM¹⁶, we assume that Au grows on (111) crystalline directions, except for the first few layers near the interface that may present some disorder.

FIGURES



FIG. 1. r-space distribution for Au(111). 5th layer (close to the surface),

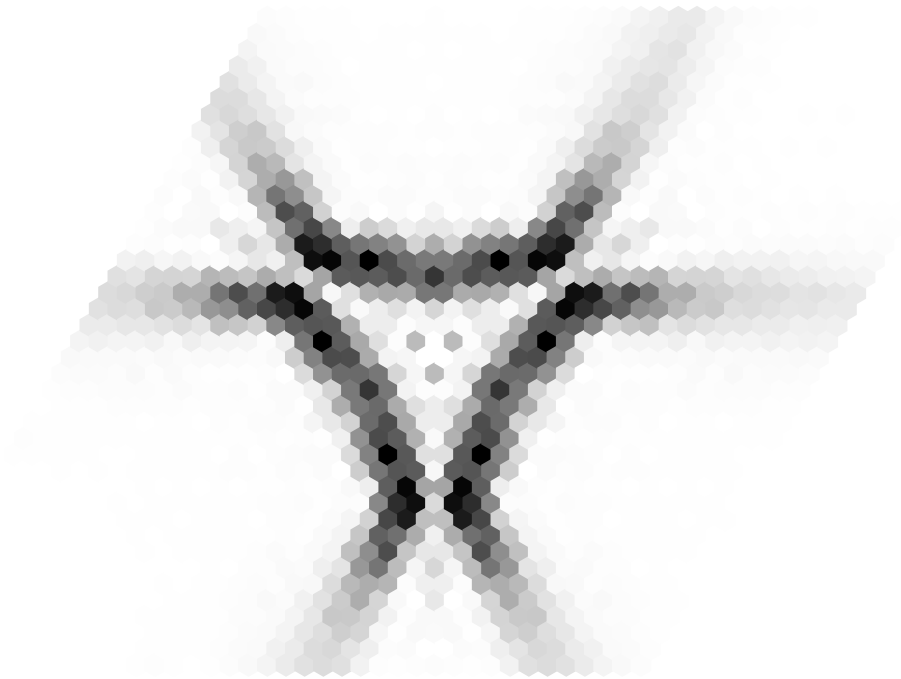


FIG. 2. r -space distribution for Au(111). 15th layer (far from the surface).

First of all, we observe the formation of narrow beams and lines in real space (e.g. see Figs. 1 and 2). This effect was previously predicted on the basis of a semi-classical calculation of the Green's functions necessary to compute Eq. 3⁸, and it is now confirmed working with a more accurate, full quantum mechanical, approximation based on a decimation technique¹⁷. The same effect has also been observed when the propagation of electrons on (100) directions is considered⁹. In fact, within our formalism, it is possible to follow the propagation through the material layer-by-layer. In this way, we can observe the gradual construction of Bloch states inside the solid, seen in particular by the formation of gaps in characteristic directions

like the (111) or (100) depending on the energy. This is the case when Figs. 1 and 2 are compared: close to the surface (1) electrons spread in all directions (including the (111)), but far away (2) the propagation in that direction is inhibited.

Secondly, we study the current distribution in k-space (e.g. see Fig. 3). In the purely elastic case, the energy is a real quantity and the wavefunction does not decay. However, it is usual in any Green's function formalism to add a very small imaginary part to the energy to create a region in the complex plane free of poles to ensure the proper analytic behaviour. In this work, we discuss the case of a very small imaginary part added to the energy ($\eta = 0.001$ eV), while we leave a detailed discussion of a finite η , representing electron-electron inelastic interaction, for a forthcoming paper¹⁸. A typical current distribution under these conditions can be seen in Fig. 3. This distribution does not present noticeable changes when observed at different layers. The symmetry found is six-fold, also obtained on other similar quantum-mechanical calculations¹³. This result is expected because these currents reflect the projected density of states on a given layer. It is interesting to notice, however, the different symmetry found in real space (three-fold), reflecting the symmetry of the whole lattice.

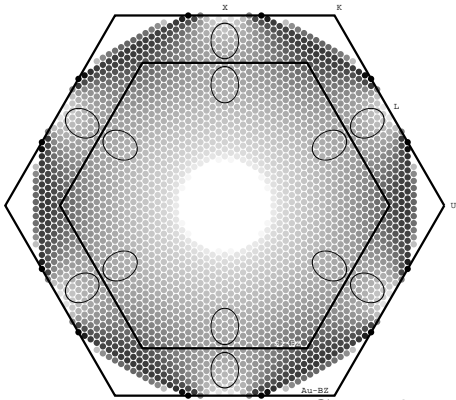


FIG. 3. k-space distribution for Au(111), $\eta=0.001$ eV.

B. Spectroscopy: Au on Si(111) and Si(100).

An interesting feature of BEEM is its ability to bring spectroscopic information of the interface. A very simple model shows how the spectroscopy is an integral on energies of different factors². Therefore, the different dependences with energy of these factors can be checked against the experiment through comparison of $I(V)$ curves.

We apply our formalism to compute the $I(V)$ curves of the Au/Si(111) (75\AA) and Au/Si(100) (100\AA) taken at low temperature (77 K)^{3,19}. These are favourable cases to be compared with a pure elastic theory, and in some way mark the correctness of the name ballistic given to the technique: from a direct comparison between experiment and theory (e.g. see Fig. 4) we conclude that the ballistic assumption breaks down at voltages higher than 1.3 eV. The theory has been calculated using k-space distributions like the ones shown in Fig. 3, with a very small η (0.001 eV), and assuming that the electrons are injected only in the first pass. The introduction of an electron-electron inelastic interaction has the main effect of taking out intensity due to the important loss involved (typically half of the energy is lost). In Fig. 4 we also show the effect of introducing such a finite η to match the ballistic intensity to the experiment. Our best fit has been obtained using the energy dependence proposed by Bell³ and for a mean free path of 155\AA at 1 eV. While not a particular effort to optimize these values has been made, both $D = 75\text{\AA}$ and $D = 300\text{\AA}$ can be explained at the same time using this approach. It is worth commenting that the standard mean free paths values derived from the gas electron theory²⁰ cannot describe correctly the data

because apparently underestimate the electron-electron interaction resulting in longer mean free paths. Finally we should comment on the role of the multiple reflections inside the metallic layer. As mentioned above, the ballistic result is obtained from direct injection, but in a more appropriated description multiple reflections must be taken into account, as shown by Bell³. Because mean free paths are longer at lower energies their effect is more important near the threshold, but on average for a width like $D = 75 \text{ \AA}$ three to four reflections are enough. This brings about the model for reflections at the surface and at the interface. We have considered perfectly specular reflection and completely diffuse reflection: differences are not dramatic because of the focusing effects introduced by the lattice, but the diffuse reflection model produces the best agreement with the experiments.

Figure 3a

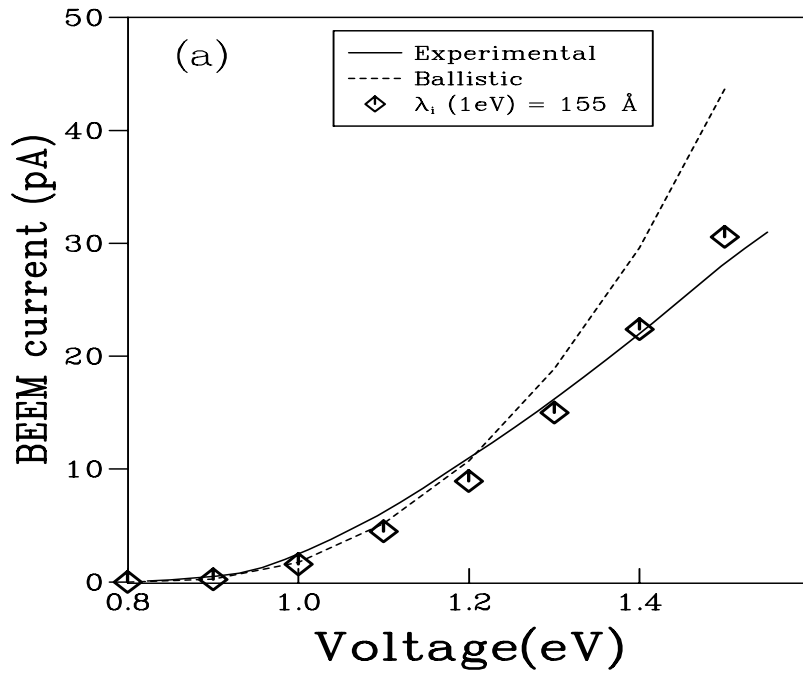


FIG. 4. IV curve for Au on Si(111) under ballistic conditions (dashed line), and including inelastic effects (rhombes), compared to experimental results (solid line) as measured by Bell in ref. [3] ($D=75$ Å, $T=77$ K).

Figure 3b

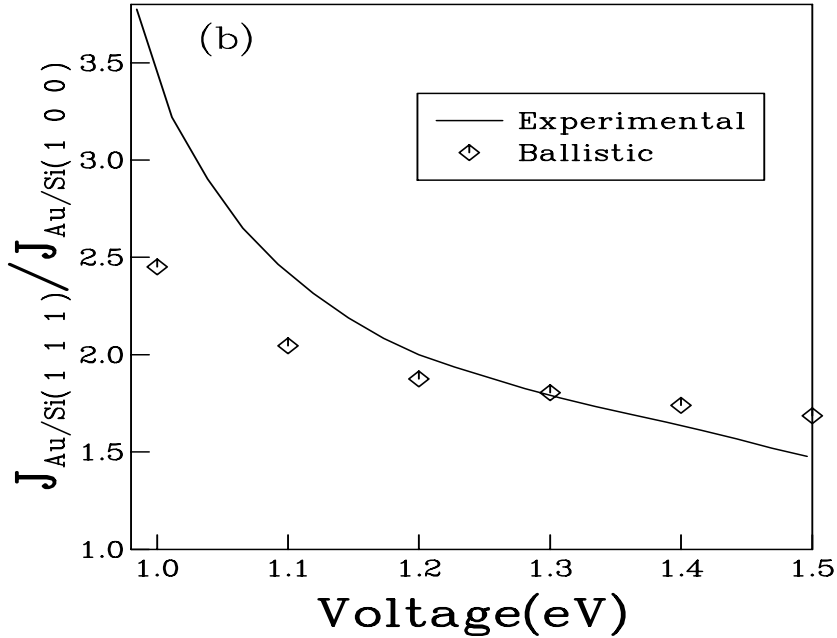


FIG. 5. Comparison between BEEM currents for Au on Si(111) ($D=75 \text{ \AA}$) and Au on Si(100) ($D=100 \text{ \AA}$). Solid line: experimental data from references [3] and [19]. Rhombes: $J(100)/J(111)$ computed from a ballistic theory.

In the past, it has been difficult to understand why Au/Si(111) and Au/Si(100) produced so similar BEEM currents in spite of their different projected band structure. This is specially difficult without realizing that the elastic interaction of electrons with the lattice results in k -space current distributions that accumulates around the two-dimensional Brillouin zone edge. To test the similarity between the two interfaces we compare in Fig 5 our results for the two orientations with the experiments. The ratio between the intensity for

the 111 orientation to the intensity for the 100 orientation is plotted against the tip voltage. The same trend is clearly observed in theory and experiment, and the main discrepancy (about $\frac{30}{100}$) is seen for low voltages, where the different Schottky barrier for the two orientations produce a bigger uncertainty on the comparison. This clearly shows how the different projected band structure of the two orientations for silicon yields similar BEEM-currents without having to resort to non-conserving parallel momentum due to scattering processes of the electrons at the interface²¹.

IV. CONCLUSIONS

We present an *ab initio* theory based on Green's functions techniques and a tight-binding hamiltonian to compute the current distributions for a BEEM experiment in real and reciprocal space. Focusing of the propagating electrons is determined by the elastic interaction with the periodic lattice. The resulting narrow lines and beams are of the order of 2-3 atomic interspacing, explaining the observed nanometric resolution of the technique. In reciprocal space we observe a six-fold distribution that determines the pure ballistic current. Comparison of experimental results taken on thin layers and at low temperature with the elastic theory ($\eta = 0.001$ eV) shows the influence of inelastic processes in the high energy range (≈ 1.5 eV). Finally, an inelastic electron-electron interaction is taken into account resulting in a good agreement between the theory and the experimental data.

V. ACKNOWLEDGMENTS

We acknowledge financial support from the Spanish CICYT under contracts number PB94-53 and PB92-0168C. K.R. is grateful for financial support from SFB292 (Germany). We are grateful with Prof. P. Kocevar and Dr. U. Hohenester for many interesting discussions and their effort to build a *first-principles* k-space Monte-Carlo approach to the BEEM problem, and with Prof. K. Heinz for his continued interest.

REFERENCES

- ¹ W.J. Kaiser and L.D. Bell, Phys. Rev. Lett. **60** 1406 (1988); L.D. Bell and W.J. Kaiser, Phys. Rev. Lett. **61** 2368 (1988);
- ² M. Prietsch, Physics Reports, **253**, 164 (1995).
- ³ L.D. Bell, Phys. Rev. Lett. **77**, 3893 (1996).
- ⁴ U. Hohenester and P. Kocevar, private communication; U. Hohenester, P. Kocevar, P. de Andres, F. Flores, Proc. 10th Conf. on Microscopy of Semiconducting Materials MSM-X (Oxford 1997), Ed. T. Cullis, in print.
- ⁵ J.B. Pendry, *Low Energy Electron Diffraction*, Academic (London, 1974).
- ⁶ D.A. Papaconstantopoulos, *Handbook of the Band Structure of Elemental Solids* (Plenum, N.Y. 1986).
- ⁷ L.V. Keldysh, Zh. Eksp. Teor. Phys. **47** 1515 (1964); Sov. Phys. JETP **20** 1018 (1965).
- ⁸ F.J. Garcia-Vidal, P.L. de Andres, and F. Flores, Phys. Rev. Lett. **76**, 807 (1996).
- ⁹ P.L. de Andres, F.J. Garcia-Vidal, D. Sestovic, F. Flores, Phys. Scr. **T66**, 277 (1996).
- ¹⁰ A. Martin-Rodero, F. Flores and N.H. March, Phys. Rev. B, **38**, 10047 (1988)
- ¹¹ F. Flores, P.L. de Andres, F.J. Garcia-Vidal, L. Jurczyszyn, N. Mingo, and R. Perez, Prog. Surf. Sci., **48**, 27 (1995).
- ¹² R. Ramirez, M. C. Böhm, Int. J. Quantum Chem., **30**, 391 (1986).
- ¹³ M.D. Stiles and D.R. Hamann, Phys. Rev. Lett. **66**, 3179 (1991).
- ¹⁴ M. Elices, F. Flores, E. Louis, J. Rubio, J. Phys. C **7**, 3020 (1974)
- ¹⁵ F. Garcia-Moliner, F. Flores *Introduction to the theory of solid surfaces*, Cambridge Univ. Press, 1979 (Cambridge).

- ¹⁶ K. Oura and T. Hanawa, Surf. Sci. **82**, 202 (1979); A.K. Green and E. Bauer, Journal of Appl. Phys. **47**, 1284 (1976); M.T. Cuberes *et al.*, J. Vac. Sci. Technol. B **12** (4), 2422 (1994).
- ¹⁷ F. Guinea, C. Tejedor, F. Flores, E. Louis, Phys. Rev. B **28**, 4397 (1983).
- ¹⁸ K. Reuter *et al.*, in preparation.
- ¹⁹ L.D. Bell, M.H. Hecht, W.J. Kaiser, Phys. Rev. Lett. **64**, 2679 (1990).
- ²⁰ J.J. Quinn, R.A. Ferrell, Phys. Rev. **112**, 812 (1958).
- ²¹ R. Ludeke and A. Bauer, Phys. Rev. Lett. **71**, 1760 (1993).